

## The ‘skin effect’ of subsurface damage distribution in materials subjected to high-speed machining

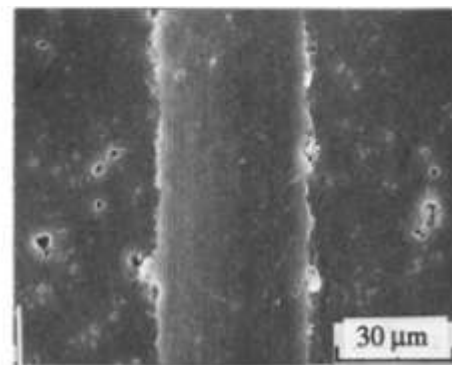
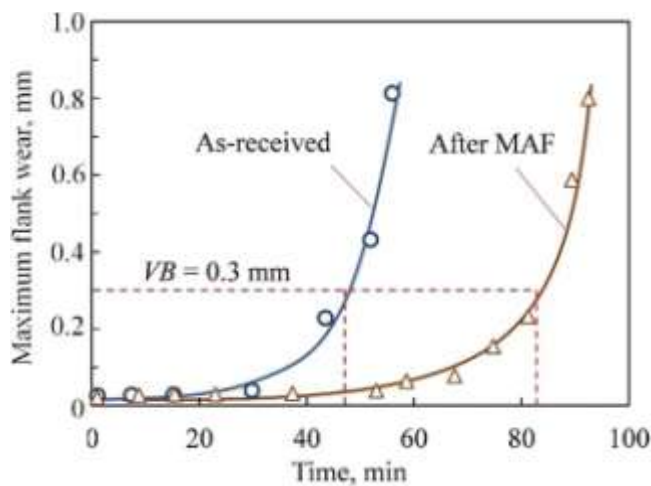
<sup>1</sup>satchidananda Ghosh, <sup>2</sup>subham Kumar Dash  
Gandhi Institute of Excellent Technocrats, Bhubaneswar, India  
Capital Engineering College, Bhubaneswar, Odisha, India

### ABSTRACT:

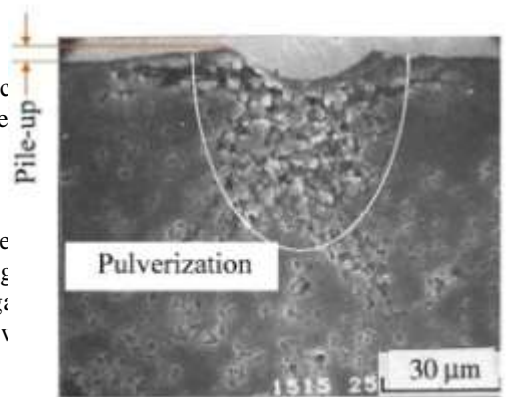
This paper proposes the ‘skin effect’ of the machining-induced damage at high strain rates. The paper first reviews the published research work on machining-induced damage and then identifies the governing factors that dominated damage formation mechanisms. Among many influential factors, such as stress-strain field, temperature field, material responses to loading and loading rate, and crack initiation and propagation, strain rate is recognized as a dominant factor that can directly lead to the ‘skin effect’ of material damage in a loading process. The paper elucidates that material deformation at high strain rates ( $>10^3 \text{ s}^{-1}$ ) leads to the embrittlement, which in turn contributes to the ‘skin effect’ of subsurface damage. The paper discusses the ‘skin effect’ based on the principles of dislocation kinetics and crack initiation and propagation. It provides guidance to predicting the material deformation and damage at a high strain-rate for applications ranging from the armor protection, quarrying, petroleum drilling, and high-speed machining of engineering materials (e.g. ceramics and SiC reinforced aluminum alloys).  
Keywords: skin effect, strain rate, dislocation, embrittlement, damage

### INTRODUCTION

The term ‘skin effect’ has been used to describe distribution of the alternating current in a conductor that electric current mainly flows in the ‘skin’ layer of the conductor. The current density is the highest at the surface layer of the conductor and quickly decreases in the inner layers. The ‘skin effect’ is further strengthened at a higher frequency of the alternating current. Similarly, the authors have found that the ‘skin effect’ of subsurface damage (SSD) distribution also exists in material deformations. The ‘skin effect’ of SSD distribution can be enhanced at a higher strain rate in a loading process. Generally, an increased strain-rate results in embrittlement of the materials subjected to loading, which in turn leads to the ‘skin effect’. For example, in armor applications, the brittleness of the material greatly affects the ballistic performance of an armor. Ceramics generally have better resistance to the ballistic impact than metallic materials [1,2]. Another example is the high-speed machining (HSM) of engineering materials, such as ceramics and SiC reinforced aluminum alloys. High speeds of machining could embrittle the workpiece material and suppress SSD depth because of the ‘skin effect’. We are living in a world that needs support from various materials. How these materials may serve our purposes has been a subject of study. Some materials are harder and more



(a) Top view



(b) Cross-sectional view

Figure 1. Maximum flank wear of the different tool inserts versus mac  $\mu\text{m}/\text{rev}$ , depth of cut: 1.0 mm, coolant: 5% vol. tri solution). Reprint from Elsevier.

brittle (e.g. ceramics, semiconductors, cast irons) than others (e.g. materials into various products with the help of modern manufacturing technologies, such as machining, laser beam cutting, forming, forging; to perform the functions as they may include strength and toughness, fatigue strength (e.g. aircraft engines and bridges), wear resistance (e.g. bearings and cutting tools), etc. To achieve the right materials must be chosen for the appropriate applications.

Titanium, Inconel, and aluminum alloys, for example, are normally used in the aerospace applications [3,4]. Crystalline silicon is a typical substrate material for the semiconductor [5–7] and photovoltaic industries [8,9]. Sapphire is used as the substrate material for LEDs [10–12]. Ceramics have been used in the high-precision bearings and cutting tools [13,14].

Glasses are indispensable materials for optics and light transmission [15]. However, the above-mentioned materials can easily be induced with SSD when they are subjected to machining.

In machining of titanium, Inconel and aluminum alloys, work hardening and tool wear are notable, resulting in a metamorphic layer on the machined surface [16–19]. Generally, the metamorphic layer degrades the service performance of a

part because of the different mechanical properties from the bulk material, such as hardness, toughness, and plasticity [20, 21]. On the other hand, materials, such as SiC, sapphire, and silicon, are hard and brittle, and can easily be introduced with SSD during a machining process [7, 15, 22], which is detrimental to the performance and lifetime of a part.

As shown in figure 1, an as-received cutting tool insert offered a lifetime of approximately 49 min. However, when another insert of the same batch from the same manufacturer was finished by the magnetic abrasive finishing (MAF) technique, its lifetime was 86 min, almost doubling the lifetime of the as-received version. Why should this happen? What is the function of MAF on the lifetime of the insert?

Figure 2. SEM images of (a) top view and (b) cross-sectional view of a smooth groove generated by grinding in an alumina sample. [24] (1988) © Chapman and Hall Ltd. With permission of Springer.

To answer these questions, an early work conducted by Zhan et al [24,25] should be referred to. In their work, Zhan et al produced a smooth groove in a hot-pressed alumina sample in the single-point grinding process at a speed of  $1800 \text{ m min}^{-1}$ . Figure 2 shows the images of the groove taken from the top and cross-sectional views by a scanning electron microscope (SEM). Figure 2(a) presents the top view of the groove with a smooth surface. Although the groove did not show any observable damage (e.g. cracking, chipping), its

subsurface was severely damaged with a layer of pulverization, as shown in figure 2(b). Moreover, the cross-sectional view reveals that material pile-up occurred to the two sides of the groove. The pile-up was clearly because of the side flow of the pulverized material. Therefore, pile-up does not have to be plastic deformation in the machining of the hard and brittle materials.

Based on the understanding of figure 2, it is suggested that the cutting edge of the as-received insert in figure 1 should have been left with the grinding-induced SSD which is responsible for the compromised tool life. Upon the removal of SSD by the MAF technique, tool life was largely extended, as depicted in figure 1. Therefore, the removal of the machining-induced damage is beneficial to the improvement of the performance and lifetime of a cutting tool. Over the years, continuous efforts have been made in machining of hard and brittle materials. Bifano et al [26] were

the first to propose the 'ductile-regime' machining technique for brittle materials to achieve high-quality grinding. presented in equation (1) [46,47],

Although 'ductile-regime' machining has received much attention, it is still controversial as it lacks both theoretical and experimental support. This technique is mainly concerned

$$\frac{de}{dt} = \frac{V \cos \alpha}{D \cos(\alpha - \gamma)} \quad (1)$$

with surface finish with no consideration of SSD of a machined workpiece. It has not solved the machining problems of the hard and brittle materials.

In order to solve these problems, Zhang et al [25] used a different approach. They not only investigated the surface but also the subsurface characteristics of a machined workpiece.

where the elemental chip thickness is related to the depth of cut. However, equation (1) cannot be used to calculate the strain rate in the machining of hard and brittle materials because these materials do not normally show notable plastic deformation before fracturing. Wang et al proposed a simple formula for calculating strain rate, shown as equation (2) [48],

$$\frac{de}{dt} = \frac{V}{a_c} \quad (2)$$

been applied in industry for high efficiency and low damage machining of ceramic materials.

Ultrasonically-assisted machining (UAM) has successfully been used in reducing machining force and improving surface integrity for the hard and brittle materials [31–35]. In fact, UAM helps suppress machining-induced damage,

enhance the critical depth of cut [31], reduce machining forces [32,36], and alter material properties [37]. UAM has a great potential for machining of the hard and brittle materials, however, there are still critical issues to be resolved. The issues include how UAM suppresses the machining-induced

where  $a_c$  represents depth of cut. Equation (2) describes strain rate in the region of a material compressed by a cutting tool. In this study, equation (2) is adopted to calculate strain rate based on the previous studies. As shown in figure 3, the SSD

depth in the hard and brittle materials decreases with an increase in strain rate of machining, which well depicts the 'skin effect' of damage formation in terms of strain rate. The best fitting line in figure 3 shows that the SSD depth is mathematically proportional to the negative exponent of strain rate, as presented in equation (3),

damage and improves workpiece surface integrity.

HSM has attracted much attention because of its improvement in machining efficiency, reduction in tool wear,

$$d = k \cdot \left( \frac{de}{dt} \right)^{-0.34} \quad (3)$$

(3)

and suppression in workpiece damage as compared to the conventional machining [38–40]. HSM can be applied to many different materials with no specific requirements on the workpiece properties. Most of all, HSM leads to a high strain rate which results in the so-called 'skin effect', namely, the machining-induced SSD tends to distribute in the superficial layer of a workpiece machined at a high strain rate [41–45]. Therefore, HSM presents a huge potential in high-efficiency machining of the above-mentioned materials. However, the underlying mechanisms of the 'skin effect' of SSD distribution remain unrevealed and need investigations. This paper is to explore the mechanisms of the 'skin effect' of SSD at high strain rates and its application to HSM. Among the differences between HSM and the low-speed machining, the strain rate is the primary factor. This paper presents the 'skin effect' of SSD distribution at high strain rates ( $>10^3 \text{ s}^{-1}$ ) with section 2 dealing with the 'skin effect' of machining-induced damage. Section 3 discusses the underlying mechanisms of the 'skin effect' at high strain rates; section 4 discusses the 'skin effect' in terms of dislocation and energy theories; section 5 concludes the paper and presents an outlook.

### 1. 'Skin-effect' of damage at high strain rates

In machining, the plastic strain rate  $d\varepsilon/dt$  is regarded as a function of rake angle  $\gamma$  of a cutting tool, shear angle  $\phi$ , cutting speed  $V$ , and the elemental chip thickness  $\Delta y$ , as where  $k$  is a constant ( $k=1531$  in figure 3).

In addition, the 'skin effect' can also be found in the metallic materials. The 'skin effect' was identified in the early works conducted on IN-718 by Pawade et al [60], on the nickel-based FGH95 superalloys by Jin et al [42, 43], on the D2 tool steels by Kishawy and Elbestawi [61], and on the nickel-based ME16 superalloys by Veldhuis et al [62]. Therefore, the 'skin effect' exists not only in the hard and brittle materials, such as ceramics, semiconductor materials, and glasses, but also in the metallic materials, such as superalloys and tool steels.

The 'skin effect' is an intrinsic property that governs the damage behavior of the engineering materials. The 'skin effect' can be interpreted as 'material damage (e.g. cracking, dislocation, phase transformation) is localized if the material is loaded at a high strain rate'. In the case of machining, for example, SSD depth decreases at an increased machining speed (strain rate), and vice versa.

### 2. Mechanisms of the 'skin-effect' of damage at high strain rates

#### Material embrittlement

Generally, a material subjected to machining undergoes plastic deformation before it fractures. The plastic deformation is governed by dislocation motion which is dependent on strain and strain rate. The relationship between the dislocation motion and strain rate is inferred based on the Orowan theory

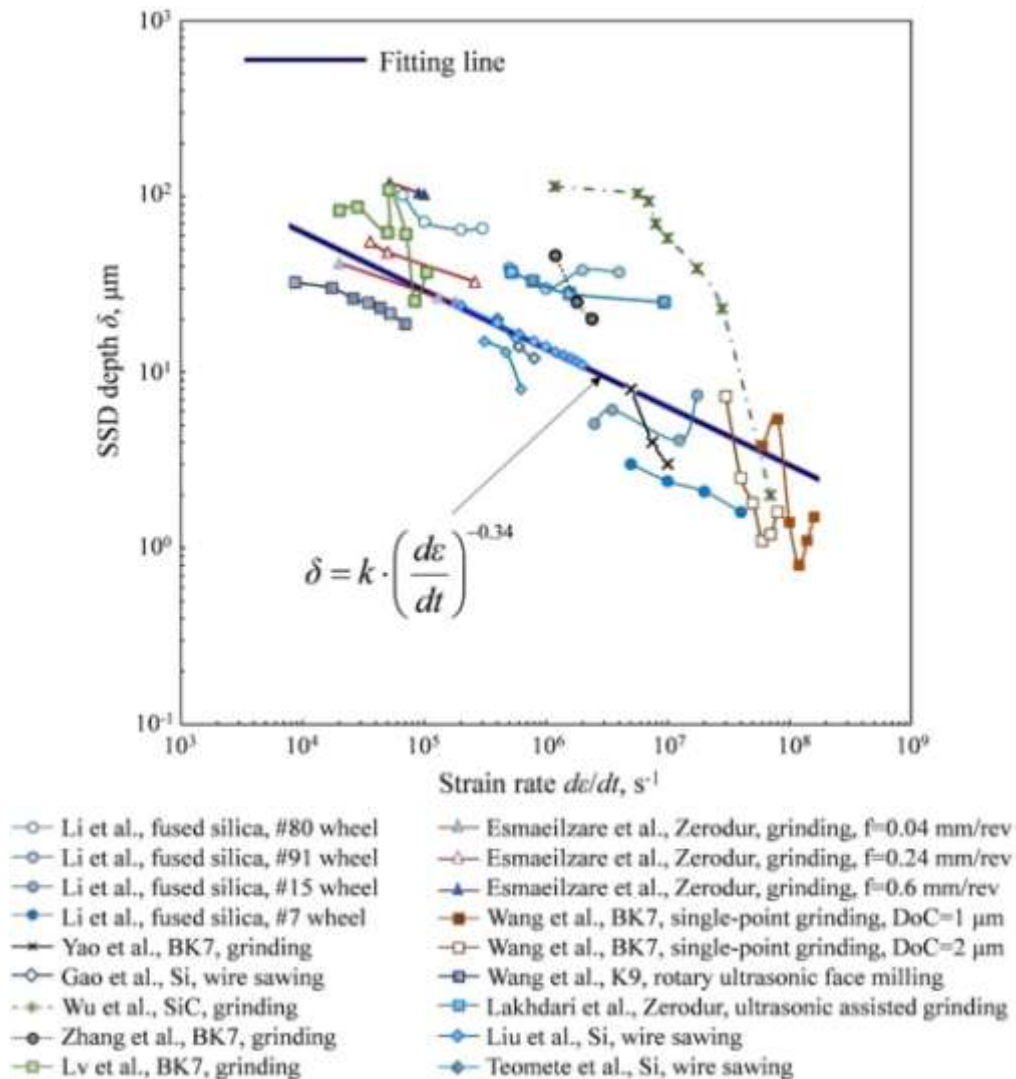


Figure 3. SSD depth of the hard and brittle materials at different strain rates in machining [22, 49–59]. Other conditions are provided in the

figure legends.

[63], as given in equation (4),

$$\frac{d\varepsilon}{dt} = r b v,$$

(4)

Therefore, the strain rate in machining is obtained as

$$\frac{d\varepsilon}{dt} = \frac{dr}{dt} b L + r b v,$$

(7)

$$\frac{d\varepsilon}{dt} = \frac{dr}{dt} b L + r b v,$$

where  $\rho$  is dislocation density;  $b$  is the magnitude of the Burger's vector; and  $v$  is dislocation velocity [64, 65]. However, equation (4) only describes an instantaneous motion of a dislocation excluding the dynamic behaviors, such as nucleation, immobilization, recovery, and annihilation. Therefore, a more adequate model is needed. Strain can be calculated by

where  $\frac{d\rho}{dt}$  is the change rate of dislocation density. The right side of equation (7) has two terms, the first term representing the nucleation and annihilation of dislocations and the second term representing dislocation movement [67]. The dislocation velocity  $v$  can be resolved by the applied shear stress [67]

equation (5)[66],

$$Cv=bt,$$

(8)

$$e=rbL,$$

(5)

where  $C$  is the drag coefficient due to lattice viscosity and  $r$  is

where  $L$  is the average displacement of a dislocation. Then, the relationship between the dynamic behaviors of dislocations and strain rate can be inferred by differentiating both sides of equation (5), the applied shear stress. As shown in figure 4, the dislocation velocity increases with the applied shear stress, but by an upper limit. The dislocation velocity is bounded by the phonon drag effects [67–70] with the time between obstacles [71], the dislocation velocity does not exceed the sound velocity in the

$$\frac{de}{dt} = \frac{d(rbL)}{dt} = r \frac{dbL}{dt} + rb \frac{dL}{dt},$$

(6)

material [72,73]. At a strain rate high enough to the extent

that the moving dislocations cannot effectively accommodate

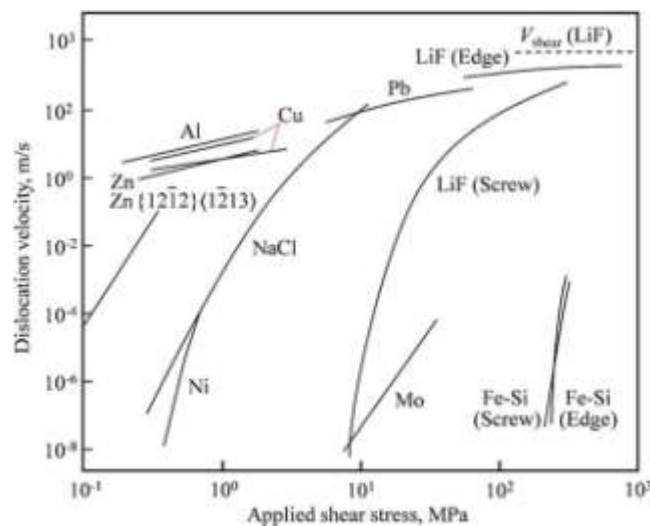


Figure 4. Relationship between dislocation velocity and applied shear stress for different materials. [74] John Wiley & Sons. ©1994 WILEY-VCH Verlag GmbH & Co. KGaA, Weinheim.

yield-to-tensile ratio  $\sigma_y/\sigma_b$  increases. At a high strain rate ( $>10^4 \text{ s}^{-1}$ ), the yield strength approaches the tensile strength. As a limit, the yield strength can be the same as but never surpass the tensile strength [76]. In this case, the material fractures prior to yielding, which is a typical characteristic of a brittle material. Material embrittlement due to the strain rate effect is thus realized.

As shown in equation (2), strain rate is determined based on cutting speed and depth of cut in the case of machining. Therefore, the strain-rate evoked embrittlement can be acquired by increasing cutting speed and decreasing depth of cut. As shown in figure 6 (a), at a cutting speed of  $1000 \text{ m min}^{-1}$ , the cutting chip exhibited a typical continuous morphology for a ductile material, such as an aluminum alloy. However, as the cutting speed increased to  $5000 \text{ m min}^{-1}$ , the chip morphology turned to be fragmental, as shown in figure 6(b), which means that the material has been embrittled under this condition.

For brittle materials, Lawn and Marshall first proposed that the ratio of hardness to fracture toughness should be used to estimate the brittleness of a material [80]. Boccacini studied the machinability of a glass-ceramics in terms of the material brittleness represented in equation (9)

$$B = \frac{H}{K_C} \quad (9)$$

where  $H$  and  $K_C$  are the hardness and fracture toughness of the material, respectively.

It should be pointed out that material hardness is strain-rate sensitive and generally increases with strain rate [16, 45, 81–85] due to the strain-rate hardening effect. A correlation between hardness and strain rate is expressed in equation (10) [86]

$$H = H_0 \left( \frac{d}{dt} \right)^m$$

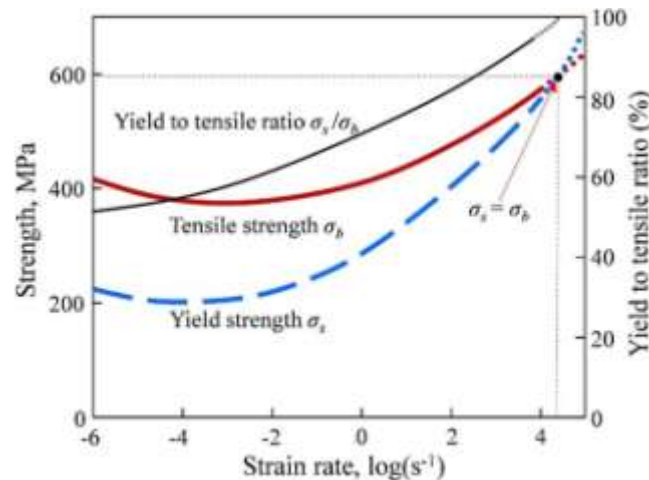


Figure 5. Strain rate dependency of material strengths [77,78].

loading, more dislocations nucleate, emitting at the sound velocity, and resulting in a dislocation avalanche. Dislocations can be classified into two types, mobile and immobile. The mobile dislocations may be trapped by each other and turned into immobile ones because of their interactions, including entanglement, attraction, obstruction, etc. Therefore, material deformation enhances not only dislocation nucleation and motion, but also dislocation immobilization. The accumulation of the immobile dislocations increases the resistance to plastic deformation and leads to material hardening [75]. At a high strain rate, dislocation avalanche may dramatically increase the density of the immobile dislocations which are responsible for material hardening. Consequently, the plastic deformation of a material is suppressed before fracturing, namely, the material is embrittled. In terms of the strength enhancement, both tensile strength  $\sigma_b$  and yield strength  $\sigma_y$  increase with strain rate, as shown in figure 5. However, as strain rate increases, the yield stress increases more rapidly than the tensile strength and the

where  $m$  represents strain-rate exponent, and  $m = 0$  for a rigid-perfectly plastic material and  $m = 1$  for a linear viscoelastic solid, respectively [87,88]. Hardness has a power law dependence on strain rate.

The variation in fracture toughness is complicated. Machado et al found that the fracture toughness of

CFRP decreased as strain rate increased [89, 90]. Anton et al found that the dynamic fracture toughness of the Pyrex glass was greater than the static fracture toughness. However, for the magnesium partially-stabilized zirconia and yttria-tetragonal zirconia polycrystals, the dynamic fracture toughness was smaller than the static fracture toughness [91]. Generally, the fracture toughness of a material is larger at a high strain rate than under the static or quasi-static condition. Suresh et al found that the ratio of the dynamic to static fracture toughness was in the range of 1.1–1.6 for brittle ceramics [92]. Liu et al studied the high-speed grinding of silicon carbide ceramics and concluded that the dynamic fracture toughness was related to strain rate [93]. Even if both the hardness and fracture toughness increase with strain rate, the former demonstrates a higher rate of increase than the latter. Therefore, as the strain rate increases, the brittleness of a material increases accordingly.

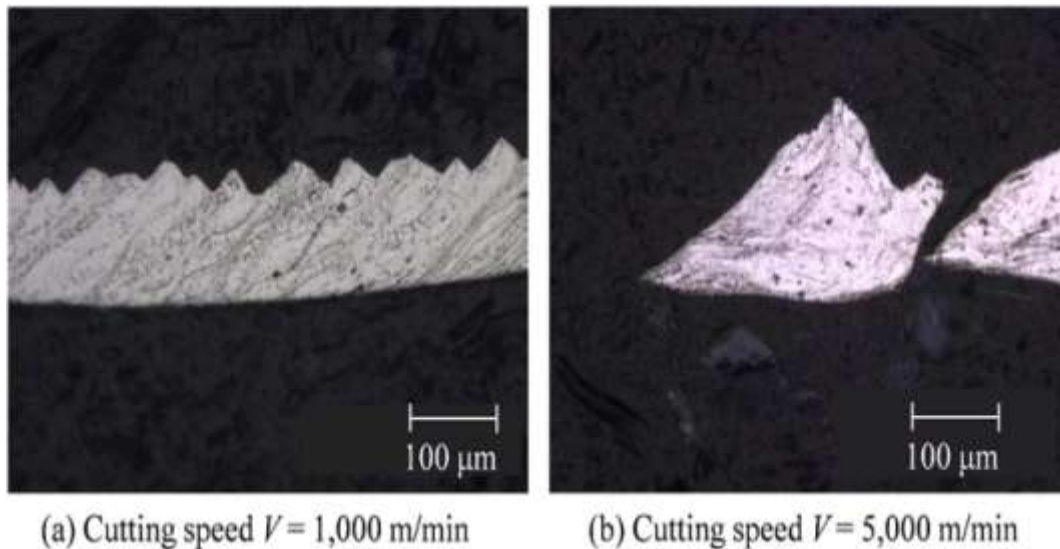


Figure 6. Chip morphologies of 7050-T7451 aluminum alloy with the uncut chip thickness of 0.1 mm and the cutting speeds (a)  $V=1000 \text{ mmin}^{-1}$  and (b)  $V=5000 \text{ mmin}^{-1}$ , respectively. Reproduced with permission from [79].

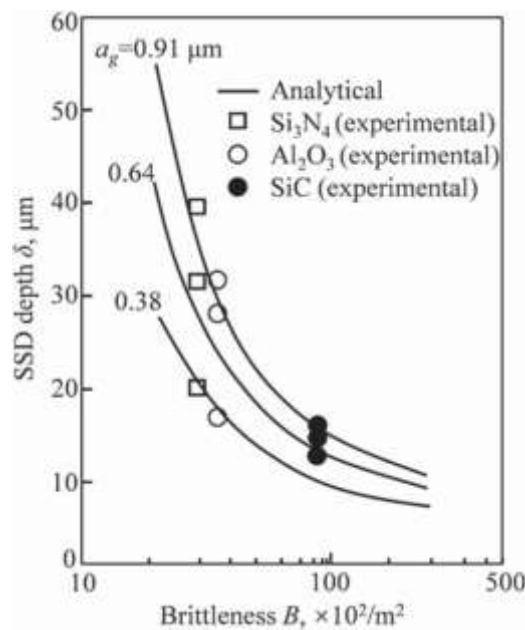


Figure 7. Variation of SSD depth with material brittleness. Reprinted from [94], Copyright (1995), with permission from Elsevier.



ZhangetalstudiedtheeffectofbrittlenessofceramicsingrindingonSSDdepthandfoundthattheSSDdepthdecreased as brittleness of ceramics increased [94], which is explained in figure 7. They presented an analytical equation for SSD depth  $\delta$  in equation (11),

#### Dislocation kinetics

Dislocations can be responsible for the formation of grain boundaries and cracks. The movement of dislocations is essential to the evolution of damage. Under an external loading condition, dislocation nucleation, multiplication, and motion are to dissipate the loading energy. The dislocations in a material may be attracted to the free surface by the image force [95–98]. As a result, the dislocation density in the skin layer of the material is higher than that in the deeper layers. In addition, dislocation density should have a larger gradient at a higher strain rate, and vice versa. If the dislocation density is not high enough to accommodate the loading from machining, for example, the dislocation entanglement should first take place in the skin layer, followed by grain refinement and cracking. Therefore, at a high strain rate, the distribution of SSD follows the 'skineffect'.

#### Stress wave effect

At high strain rates, the contribution of stress waves to the 'skineffect' of SSD distribution should be taken into consideration. As shown in figure 8, the compressive stress waves are produced due to the high speeds squeezing by a cutting tool.

The stress waves propagate along the cutting direction and they are partially reflected by the free surface because of the shortest propagation distance. The compressive stress waves can be converted to tensile stress waves from the free surface reflection, which was also described by Hopkinson [99]. Fol-

$$d = k \cdot a_g^{1/\log(\mathbf{I} \cdot \mathbf{B})},$$

(11)

lowing this line of reasoning, the reflection waves near the free surface may produce tensile stress that is unbearable for an

where  $\lambda$  are constants;  $a_g$  is the grit depth of cut. Equation (11) depicts that in grinding of ceramics, SSD depth can be suppressed by increasing brittleness of ceramics, which is obtained with an increased strain rate in high-speed grinding. In other words, the 'skineffect' of SSD distribution exists in machining of materials at an increased speed.

embrittled material. Consequently, cracks mushroom near the free surface. This may be the reason for the result that the rear portion (with stress wave reflection) were with more damage than the front portion of the samples subjected to impact loading in the study conducted by Jiangetal [100]. The impact energy is rapidly dissipated by the mushrooming of the cracks.

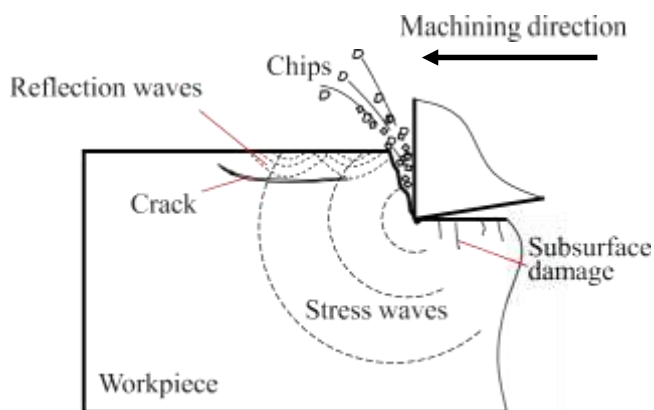


Figure 8. Schematic of stress waves propagating in the workpiece in high-speed machining.

Correspondingly, the cracks are more concentrated in than away from the surface layer of the workpiece.

#### Cracking

Generally, SSD is dependent on stress distribution. Based on the Boussinesq elastic-field theory [101], as illustrated in figure 9, there is an elastically stressed (strained)

region beneath the loading point. For an indenter with a sharp tip, the stress level approaches infinity around the tip and decreases

away from the tip. However, the stress cannot approach infinity since a material should yield or fracture as the stress exceeds the material strength. The region is subjected to hydrodynamic stress and shear stress which may result in grain refinement or pulverization.

Material damage is due to the consequence of loading during which energy is consumed by the materials subjected to loading. Damage is dependent not only on the intensity of loading stress but also on the process of loading. In other words, it is also dependent on the strain rate during loading. At an increased strain rate, the damage increases correspondingly [100, 102]. Ping et al found that the energy density in breaking a rock increased with the power law of strain rate [103]. At a high strain rate, the number of small cracks rapidly increases to effectively absorb the impact energy, the intersection of the small cracks results in the comminution of a material. Therefore, material fragmentation increases with strain rate, as shown in figure 10.

Grady proposed a model to predict fragment size, based on the balance between the kinetic energy and the newly created surface energy, as shown in equation (12) [104],

$$\left( \frac{2012 KC}{\rho} \right)^{2/3}$$

silicon, and finally the intact monocrystalline silicon [106], sequentially in the depth direction.

Figure 11 shows a schematic diagram of SSD in a brittle material subjected to machining. At the top surface is the amorphous layer below which is the pulverization layer. The pulverized material is squeezed by the cutting edge to the two sides of the groove, forming pile-up. Median and radial cracks form around the pulverization layer. If a radial crack extends to the surface, surface chipping occurs.

Stress gradient may also be responsible for the 'skineffect' of SSD. At an increased strain rate, the stress gradient increases, which may result in a concentrated SSD layer beneath the surface. As described in figure 12(a), at a low strain rate in machining, SSD depth is large and so is the chip

size. On the other hand, as the strain rate increases, the stress gradient increases, which results in more concentrated SSD in the skin layer of the material. As shown in figure 12(b), the thicknesses of the respective amorphous and pulverization layers decrease, and so does the chip size. In addition, the stress level decays faster due to a higher stress gradient, which results in a reduced SSD depth.

Based on the above analysis, figure 13 describes the distribution of SSD at different strain rates in machining. The material at the front of the cutting tool is subjected to both the deviatoric and hydrostatic stresses. In such a case, the combination of the two stresses tends to form a pulverization zone described by Zhan et al [25]. The pulverization zone consists

of microscopic cracks and an amorphous layer (or a grain-refined layer). Macro-cracks initiate and propagate from the boundary of the pulverization layer. The free surface of the

workpiece has the least resistance to crack propagation compared to the bulk material down below the surface. Therefore, based on the principle of the minimum material resistance, the crack tends to propagate toward the free surface, which leads to the damage concentration in the surface layer to cause the 'skineffect'. At an increased strain rate, as schematically shown

in figure 13(b), the chip size is decreased and the thicknesses of the pulverization and amorphous layers are reduced accordingly.

More chipping is expected in the machined surface because of the material embrittlement at the increased strain rate.

### 3. Discussion

Based on physics, SSD may be caused by lattice mismatch (e.g. dislocations and stacking faults) and bond rupture of a material. Generally, cracking can be a consequence of dislocations. For example, it may result from the accumulation and entanglement of dislocations. Therefore, at a high strain

$$d = \left( \frac{rV}{\rho} \right)^{1/3} \left( \frac{d\epsilon}{dt} \right)^{1/3} \quad (12)$$

rates, the formation and distribution of dislocations follow the 'skineffect' and so does SSD. Dislocations move toward the

wherever is the sonic velocity. The fragment size decreases at an increased strain rate [105]. The limit to the grain refinement is likely to be amorphization, as reported by Zhao et al who discovered that the microstructural change in the monocrystalline silicon under a laser-induced shock loading. The surface layer of the silicon was left with layers of micrometer-sized grains, nanometer-sized grains, amorphous free surface under the image force, creating 'skin effect', which leads to the dislocations as well as SSD accumulation near the free surface. On the other hand, high strain rate tends to promote dislocation multiplication, which in turn obstructs material deformation and causes the embrittlement to the material. Based on an early grinding study conducted by Zhang and Howes [94] on ceramic materials, SSD depth

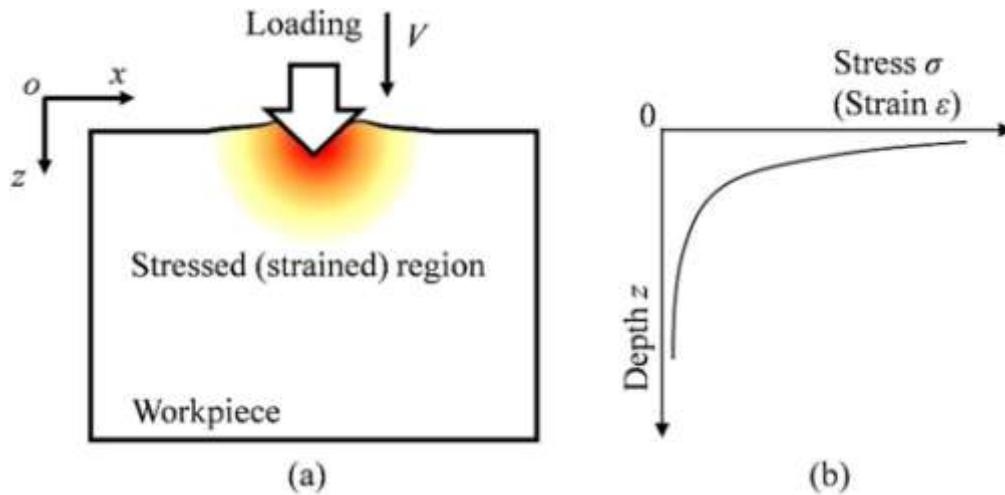


Figure 9. Schematics of (a) a stressed (strained) region around the loading point; (b) stress (strain) distribution in the depth direction.

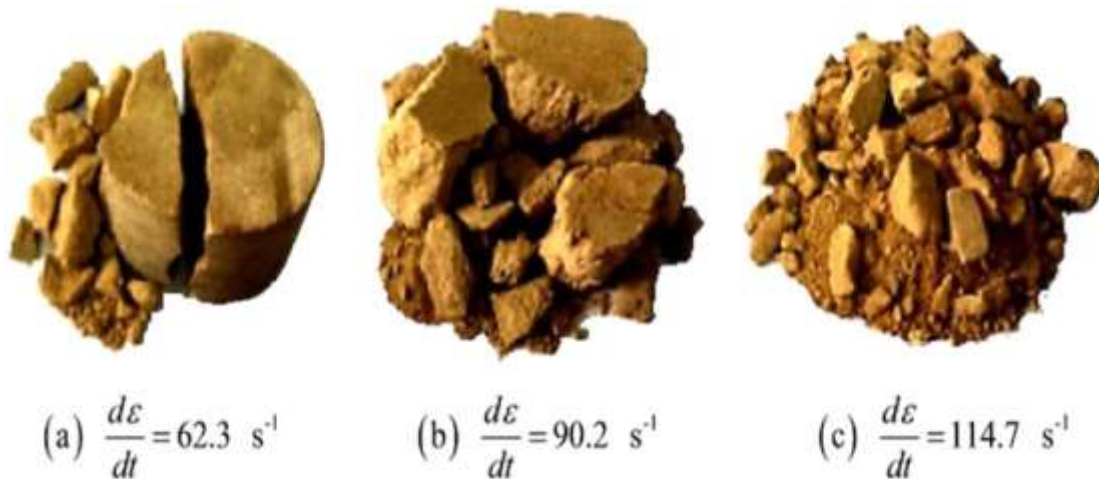


Figure 10. Fragments of sandstone impacted at different strain rates. Reproduced with permission from [102].

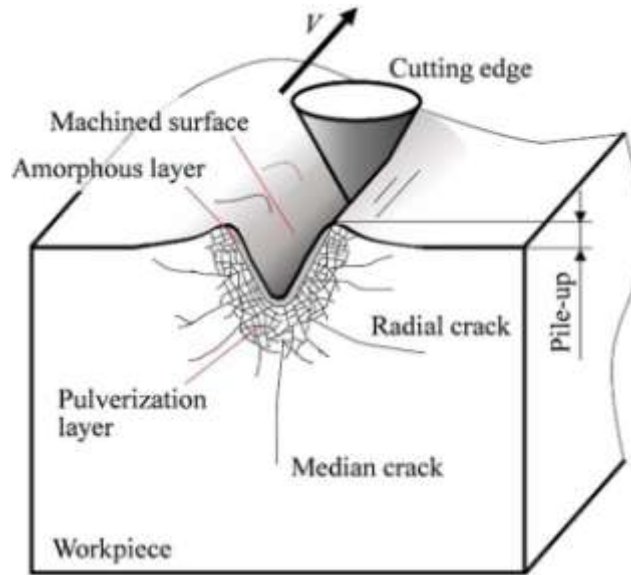


Figure 11. Subsurface damage of brittle materials.

decreases with an increase in the material brittleness. There-fore, the 'skin effect' of the dislocations and the material embrittlement due to dislocation multiplication lead to the 'skineffect' of SSD at high strain rates.

Practically, numerous factors, such as strain and strain rate, dislocation movement, crack initiation and propagation, material phase transformation, stress distribution, and stress wave propagation, as well as the changes in the material properties, are collectively responsible for the 'skineffect' of SSD. It is difficult to analyze the 'skin effect' from one factor alone. However, the effect can be comprehended from the aspect of energy dissipation.

From the energy point of view, machining is recognized as an energy rebalance process. A system with the minimum energy level is the most stable. A material in machining is activated with an elevated energy that has a tendency to transform into the most stable state of the minimum energy. The material damage, including dislocations and cracking, is a way of energy relaxation. Based on the minimum energy principle, the damage tends to move towards where the

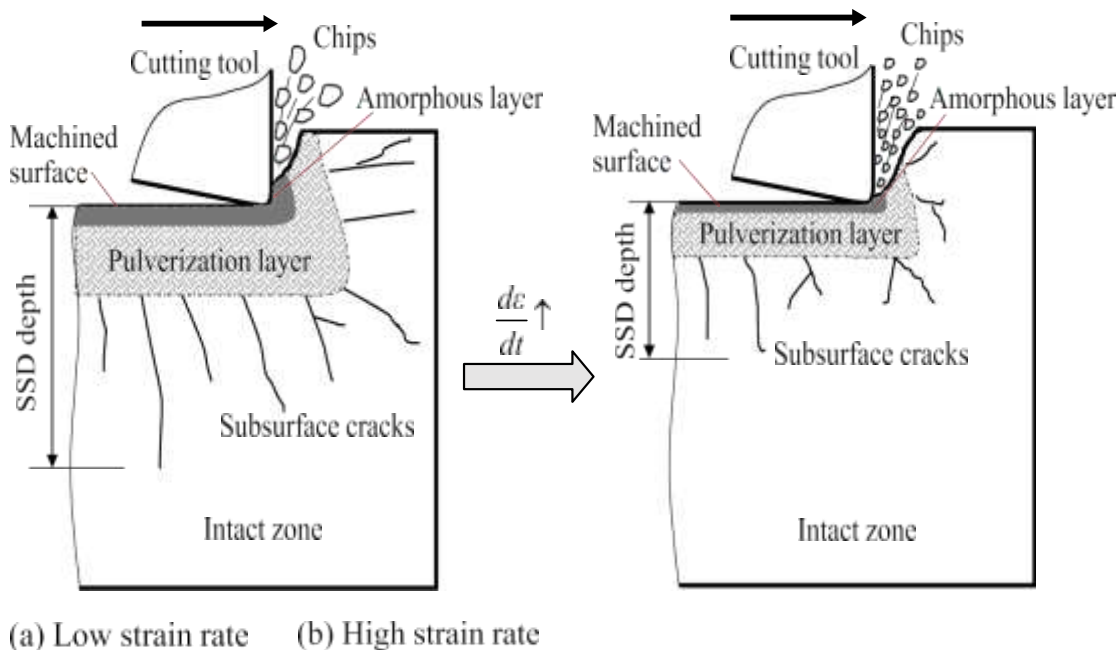


Figure 12. Subsurface damage evolution with strain rate.

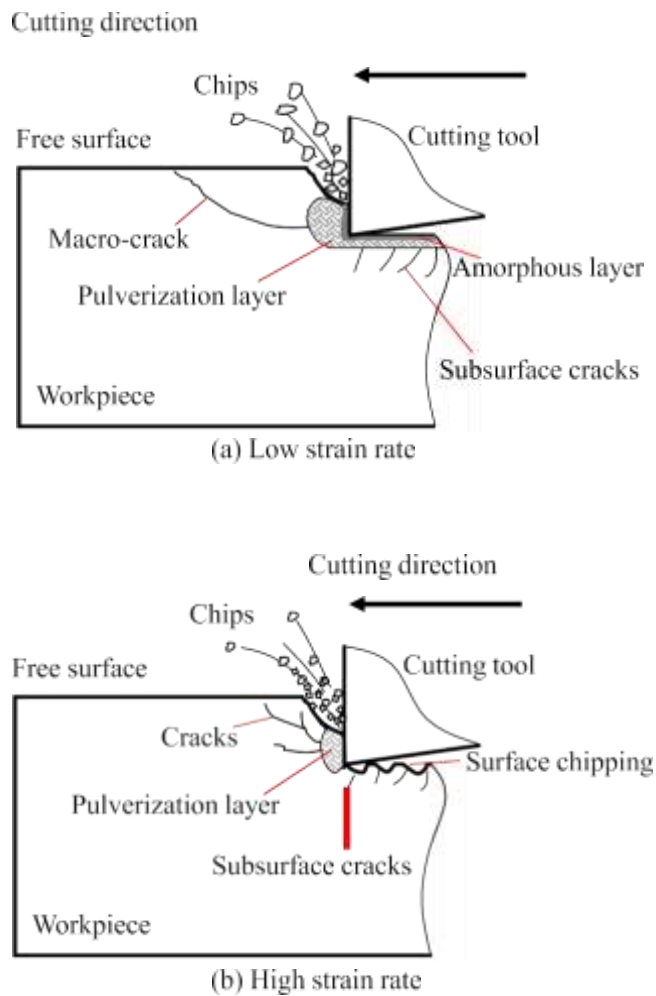


Figure 13. Propagation of macro-cracks at different strain rates.

energy requirement is the lowest for damage formation. Since the free surface has the lowest energy for damage formation compared to other locations within the material, damage tends to propagate toward the free surface.

In this paper, the effect of temperature rise on damage formation in machining is temporarily put aside to simplify the discussion. The temperature in machining indeed affects the mechanical behavior of a material, such as dislocation kinetics [107, 108], stress wave propagation, and eventually surface integrity of a machined part. Specifically, in the conventional machining of ductile materials, temperature has a notable effect on the generation of the surface metamorphic layer [17, 20, 109]. Whereas at the high strain-rate machining, the temperature effect can be neglected. The reason is expatiated in the following.

Temperature rise is a reflection of the heat generation in machining. The heat in machining of a ductile material is mainly generated from material shear and friction. However, at a high strain rate, the material is embrittled, which

directly contributes to the heat reduction from the decreased shear and friction and thus to the temperature reduction accordingly.

The 'skin effect' of damage at high strain rates provides a guidance for many industrial applications. In machining, the 'skin effect' allows to acquire the desired surface quality of a machined part by increasing strain rate in machining, such as ultrasonic assisted machining and peening.

#### 4. Concluding remarks and outlook

This paper proposes the 'skin effect' of material damage at high strain rates for the first time. The 'skin effect' is applicable not only to the hard and brittle materials, but also

to most other engineering materials, such as metallic materials. The paper draws the following concluding remarks.

- (a) The 'skineffect' of damage is obtained at a high strain rate in a loading process.
- (b) High strain rate results in an increase in material brittleness.
- (c) Brittleness is a material property that contributes to the 'skineffect' of damage in a loading process;

The 'skin effect' of damage can have numerous industrial applications. One direct application is the HSM of the difficult-to-machine materials, such as ceramics, high strength metals, and composite materials. Nevertheless, many issues remain unresolved, such as how high the stain rate should be in order to suppress SSD in machining. Other issues may include dislocation nucleation and motion, interactions among dislocations during loading at a high strain rate.

With a rapid development of the modern testing equipment and techniques, to have well-controlled testing conditions come to reality. High-speed and high-precision machine tools are readily available. In addition, the state-of-the-art characterization facilities, such as the focused ion beam device in combination with high-resolution transmission electron microscopes (HRTEM), the cathode luminescence device in combination with SEM, are also readily accessible.

With the aforementioned modern testing equipment and techniques, the unresolved issues are expected to be resolved, and the underlying physical mechanisms of the 'skin effect' of damage can further be explored in the near future.

## REFERENCES

- [1] Gao Y 2014 Study on high strain rate deformation of alumina, silicon carbide ceramics and  $Al_2O_3/SiC$  nanocomposites School of Materials Science and Technology (Beijing: China University of Geosciences)
- [2] Sternberg J 1989 Material properties determining the resistance of ceramic to high velocity penetration J. Appl. Phys. 65 3417–24
- [3] Ulutan D and Ozel T 2011 Machining induced surface integrity in titanium and nickel alloys: a review Int. J. Mach. Tools Manuf. 51 250–80
- [4] Thakur A and Gangopadhyay S 2016 State-of-the-art in surface integrity in machining of nickel based superalloys Int. J. Mach. Tools Manuf. 100 25–54
- [5] Hahn P O 2001 The 300 mm silicon wafer—a cost and technology challenge Microelectron. Eng. 56 3–13
- [6] Wang Z, Tian B, Pantouvakis M, Guo W, Absil P, Van Campenhout J, Merckling C and Thourhout D V 2015 Room-temperature InP distributed feedback laser array directly grown on silicon Nat. Photon. 9 837
- [7] Pei Z J, Billingsley S R and Miura S 1999 Grinding induced subsurface cracks in silicon wafers Int. J. Mach. Tools Manuf. 39 1103–16
- [8] Masuko K et al 2014 Achievement of more than 25% conversion efficiency with crystalline silicon heterojunction solar cell IEEE J. Photovolt. 4 1433–5
- [9] Taguchi M, Yano A, Tohoda S, Matsuyama K, Nakamura Y, Nishiwaki T, Fujita K and Maruyama E 2014 24.7% record efficiency hits solar cell on thin silicon wafer IEEE J. Photovolt. 4 96–9
- [10] Ryu H Y, Jeon K S, Kang M G, Yuh H K, Choi Y H and Lee J S 2017 A comparative study of efficiency droop and internal electric field for InGaN blue-lighting-emitting diodes on silicon and sapphire substrates Sci. Rep. 7 44814
- [11] Zang Z, Zeng X, Du J, Wang M and Tang X 2016 Femtosecond laser direct writing of microholes on roughened ZnO for output power enhancement of InGaN light-emitting diodes Opt. Lett. 41 3463–6
- [12] Lee Y J, Hwang J M, Hsu T C, Hsieh M H, Jou M J, Lee B J, Lu T C, Kuo H C and Wang S C 2006 Enhancing the output power of GaN-based LEDs grown on wet-etched patterned sapphire substrates IEEE Photonics Technol. Lett. 18 1152–4
- [13] Yin Z, Huang C, Yuan J, Zou B, Liu H and Zhu H 2015 Cutting performance and life prediction of an  $Al_2O_3/TiC$  micro-nano-composite ceramic tool when machining austenitic stainless steel Ceram. Int. 41 7059–65
- [14] Shalaby M A, El Hakim M A, Abdelhameed M M, Krzanowski J E, Veldhuis S C and Dosbaeva G K 2014 Wear mechanisms of several cutting tool materials in hard turning of high carbon-chromium tool steel Tribol. Int. 70 148–54
- [15] Li H N, Yu T B, Zhu L D and Wang W S 2016 Evaluation of grinding induced subsurface damage in optical glass BK7 J. Mater. Process. Technol. 229 785–94
- [16] Che-Haron C H and Jawaid A 2005 The effect of machining on surface integrity of titanium alloy Ti-6% Al-4% V J. Mater. Process. Technol. 166 188–92
- [17] Thakur A, Mohanty A and Gangopadhyay S 2014 Comparative study of surface integrity aspects of Incoloy 825 during machining with uncoated and CVD multilayer coated inserts Appl. Surf. Sci. 320 829–37
- [18] Herbert C, Axinte D, Hardy M and Brown P D 2012 Investigation into the characteristics of white layers produced in a nickel-based superalloy from drilling operations Mach. Sci. Technol. 16 40–52

- [19] ImranM,MativengaP,GholiniaAandWithersP2015AssessmentofsurfaceintegrityofNisuperalloyafterelectrical-discharge,laserandmechanicalmicro-drillingprocessesInt.J.Adv.Manuf.Technol.791303–11
- [20] AramcharoenA,MativengaPTandManufacturing,L.P.Group2007Whitelayerformationandhardeningeffects inhardturningofH13toolsteelwithCrTiAlNandCrTiAlN/MoSTcoatedcarbide toolsInt.J.Adv.Manuf.Technol.36650
- [21] ZhangB,ShenW,LiuY,TangXandWangY1997MicrostructuresofsurfacewhitelayerandinternalwhiteadiabaticshearbandWear211164–8
- [22] WangC,FangQ,ChenJ,LiuYandJinT2016SubsourcedamageinhighspeedgrindingofbrittlematerialsconsideringkinematiccharacteristicsofthegrindingprocessInt.J.Adv.Manuf.Technol.83937–48
- [23] YamaguchiH,SrivastavaAK,TanMA,RiverosREandHashimotoF2012MagneticabrasivefinishingofcuttingtoolsformachiningoftitaniumalloysCIRPAnn.61311–4
- [24] ZhangB,TokuraHandYoshikawaM1988Studyonsurfacecrackingofaluminascratchedbysingle-pointdiamondsJ.Mater.Sci.233214–24
- [25] ZhangBandHowesTD1994Material-removalmechanismsingrindingceramicsCIRPAnn.43305–8